PHYSICAL REVIEW C VOLUME 51, NUMBER 6 JUNE 1995

^{6}Li(π^+, pp)^{4}He$_{g.s.}$ reaction at 100 and 165 MeV incident pion energies

Z. Papandreou,* G.M. Huber, G.J. Lolos, J.C. Cormier, E.L. Mathie, and S.I.H. Naqvi
Department of Physics, University of Regina, Regina, Saskatchewan, Canada S4S 0A2

D.F. Ottewell, R. Tacik,† and P.L. Walden
TRIUMF, Vancouver, British Columbia, Canada V6T 2A3

G. Jones and R.P. Trelle‡
Department of Physics, University of British Columbia, Vancouver, British Columbia, Canada V6T 2A6

X. Aslanoglou§
Department of Physics and Astronomy, Ohio University, Athens, Ohio 45701

D.L. Humphrey
Department of Physics and Astronomy, Western Kentucky University, Bowling Green, Kentucky 42101

(Received 10 March 1995)

Differential and total cross sections for π^+ absorption on ^{6}Li leading to the $pp+{}^4$He$_{g.s}$ final state are presented at incident pion energies of 100 and 165 MeV. The narrow width of the pp angular correlation is observed and reported.

PACS number(s): 25.80.Ls, 25.80.Hp

Pion absorption has received considerable attention in the last decade due to its importance in the areas of pion-nucleus and heavy ion collisions. At incident pion energies below 1 GeV, the absorptive channel accounts for a significant portion of the total pion-nucleus cross section, and is thus of fundamental importance in understanding such interactions [1]. In addition, in heavy ion collisions where pions are created, many emerging pions are absorbed since the resonant pion mean free path in nuclear matter is only approximately 0.5 fm. In fact, in every field of investigation where pions and nuclei are in the initial and/or final state, the absorption process affects the primary physics in the reaction of interest.

It is clear, then, why such an important channel of pion-nucleus interactions has attracted experimental and theoretical investigations. Of particular interest in pion absorption on light nuclei is the contribution of absorption on $T=0$ nucleon pairs (quasideuteron absorption or QDA) and the role of more complex reactions such as absorption by three nucleons (3NA). These two channels are conceptually the easiest to investigate and understand both theoretically and experimentally, but it is not yet clear whether they alone account for the total absorption cross section, or whether other channels are involved as well. The earlier claims of a small QDA contribution to the total cross section [2] have since been revised upward when more sophisticated experiments [3,4] were performed and individual specific final states were observed after pion absorption. Such experiments have been valuable in bringing to light the different angular distributions of specific states, after such a prediction was made earlier [5] as a critique of the method used in Ref. [2].

Generally, published results on pion absorption have attempted to correct for losses due to final state interactions (FSI), either through intranuclear cascade or distorted-wave impulse approximation calculations. The accuracy of such corrections, all based on QDA plus NN interactions in the exit channel, is an open question. The emission of three protons can signify either pion absorption on a correlated three nucleon cluster, or a two-step process based on QDA plus some form of FSI of one of the primary protons with an uncorrelated nucleon in the nucleus. Such FSI corrections have been found to be very significant for pion absorption on ^{16}O [3]. On the other hand, experiments on lighter nuclei with finer detector granularity [6] have not identified a clear contribution to the data by FSI, and have excluded any measurable contribution of initial state interactions followed by proper QDA. Given the recent results from $(e,e'p)$ reactions that have claimed a longer mean free path of protons in nuclei than expected [7], the absence of clear FSI signatures in very light nuclei is not all that surprising.

^{6}Li is an attractive choice of target for pion absorption investigations because it is one of a few light nuclei that allow specific final states to be observed with medium resolution, large acceptance detectors. This nucleus has been investigated at an incident pion energy of 59.4 MeV [8], where approximately 60% of the total pion absorption cross section could be accounted for by the transition to the ground and first excited states. However, that experiment only measured one angle pair $(60°, -102.7°)$, and relied on a Monte Carlo simulation for their conclusions. Earlier results at 70 MeV

*Present address: Department of Physics, The George Washington University, Washington, DC 20052.

†Mailing address: Department of Physics, University of Regina, Regina, SK, Canada S4S 0A2.

‡Present address: Chemische Werke Bayer, Leverkusen, Germany.

§Present address: Department of Physics, University of Ioannina, Ioannina, Greece.

[9] also found that the QDA mechanism dominates the ground state and low lying ^{4}He excited state transitions. The "BGO Ball Collaboration" investigated ^{6}Li at 50, 100, 150, and 200 MeV, and extracted different charged particle multiplicities [10,11]. However, these data have limited angular information due to the coarse ($\Delta\theta = 40°$) detector granularity. The $^{6}Li(\pi^{+},pp)$ reaction was also investigated [12] at 165 MeV at KEK, and the authors claim that the broad components observed in the angular distributions are due to the two-step processes extracted from [13]. That work had good angular resolution, but was unable to extract total cross sections. Finally, the Maryland group has taken systematic measurements [14] of this reaction at 115, 140, 165, 190, and 220 MeV incident energies using NaI telescopes at three angles in coincidence with a large plastic scintillator array.

In the present work, we have investigated the $^{6}Li(\pi^{+},pp)^{4}He_{g.s.}$ reaction at incident pion energies of 100 and 165 MeV, with good angular resolution and coverage, in order to extract differential and total cross sections for the ^{4}He ground state transition. The detectors used in the present experiment have been described in detail elsewhere [15], so they will be only briefly described here.

The detectors consist of two assemblies of plastic scintillator positioned on either side of the TRIUMF M11 channel pion beam. Each assembly is further divided into two independent subassemblies, each covering 11° in the horizontal scattering plane, and $\pm 11°$ in the vertical plane. Each subassembly has a $\Delta E - E$ arrangement for particle identification, and the maximum proton stopping power is 220 MeV. Two (x,y) multi-wire proportional chambers (MWPC), in front of each assembly, were used for background rejection via two-arm trajectory extrapolation to the target. Most of the background was due to scattered pions and direct muons associated with the pion beam, and did not originate in the target. The pion flux was monitored using muon counters and in-beam plastic scintillator counters capable of counting individual muons and pions in the beam halo and in the beam itself, and was corrected for the pion beam fraction as described in [16]. The target was mounted on a target holder made of plastic scintillator, thus necessitating carbon target subtraction by measuring the ^{12}C contribution to the pp channel. However, the Q values for the (π^{+},pp) reactions on ^{6}Li and ^{12}C differ by 23.7 MeV, so the $^{4}He_{g.s.}$ transition is unaffected by the presence of the carbon in the multiple target assembly.

We have compared the data with Monte Carlo calculations using the ENIGMA [17] and GEANT codes [18]. The analysis and Monte Carlo methods will be reported in detail in a forthcoming publication on the $^{12}C(\pi^{+},pp)$ reaction [19]. Briefly, the analysis employed particle identification, trajectory reconstruction and detector reaction loss recovery techniques to reconstruct the original energy of the detected protons in the center of the ^{6}Li target. All kinematic variables discussed below have been calculated using the full trajectory reconstruction from the MWPC, with an effective resolution of 0.6° in the horizontal plane, and 1.1° in the vertical plane, including the incident pion beam divergence. However, the angular distributions are quoted for the middle of each subassembly, and thus carry an intrinsic width of $\pm 5.5°$ horizontal, and $\pm 11°$ vertical.

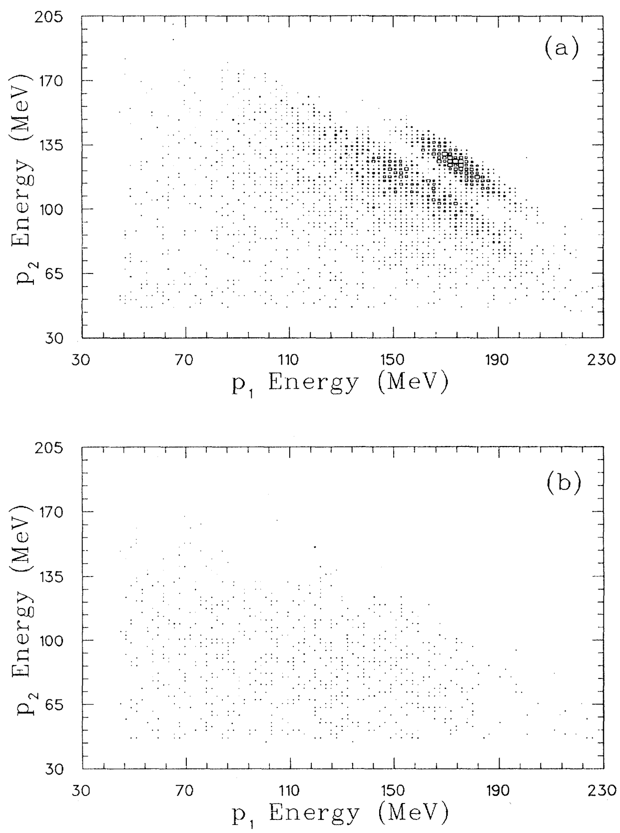

FIG. 1. Dalitz plots for the $^{6}Li(\pi^{+},pp)$ reaction at 165 MeV incident pion energy for angle pairs: (a) (54.5°, −95.5°), (b) (54.5°, −135.5°). The diagonal bands in (a) correspond to pure two nucleon absorption leading to the $pp + {}^{4}He_{g.s.}$ and $pp + {}^{4}He^{*}$ final states, while the triangular region at lower summed energy in both (a), (b) correspond to more complex absorption processes. Both (a), (b) are plotted with the same vertical scale (box size). A uniform detection threshold of 45 MeV (as calculated in the center of the target) is applied, and carbon background has been subtracted.

A representative E-E correlation (Dalitz plot) for 165 MeV incident pion energy is shown in Fig. 1(a), which is 4° from quasifree absorption (QFA) kinematics. These data have energy loss and reaction loss corrections to the flux applied. In the figure, strong energy correlations due to the ^{4}He ground and excited final states are clearly visible, showing the underlying QDA nature of the absorption process for this angle pair. Contrast this energy correlation to Fig. 1(b), which displays data taken 37° from QFA kinematics. Both Dalitz plots are normalized to the same number of incident pions and target thickness, and plotted with the same vertical scale, thus establishing the relative strength of the strongly correlated QDA protons in Fig. 1(a) with the three-body phase-space-like distribution of Fig. 1(b). The energy region far from the 2NA absorption correlation in Fig. 1(a) is very similar to the same region in Fig. 1(b), further emphasizing that the main strength in Fig. 1(a) is due to QDA, and that 3NA and multi-step processes are small components of the total in-plane reaction cross section. These figures also dem-

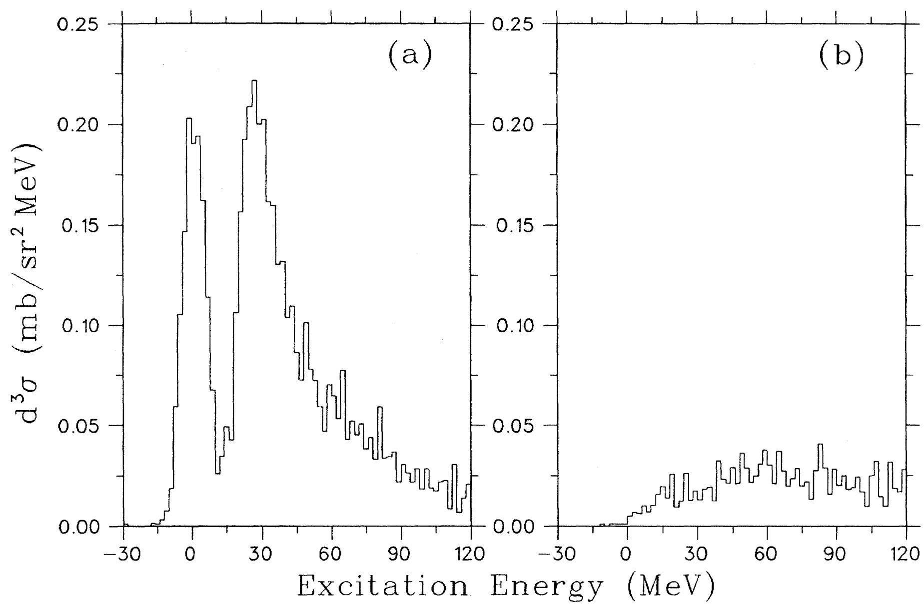

FIG. 2. Recoil excitation histograms for the same angle pairs as shown in Fig. 1. The ground state cross sections presented here correspond to those events with excitation energy between −12 and +12 MeV.

onstrate the absence of contributions under the ground state peak from $^4He^*$ or phase-space-like transitions. Excitation spectra for the same two detector configurations are shown in Figs. 2(a) and 2(b). The clear separation of the ground and excited states of ^4He is evident.

Figure 3 shows sample angular distributions for the $^6Li(\pi^+,pp)^4He_{g.s.}$ reaction at 100 and 165 MeV. The width of the pp correlation is approximately 16° full width at half maximum (FWHM) at both 100 and 165 MeV incident pion energies; this includes the finite width of the subassemblies, however, so the correlation could, in fact, be narrower. The dotted line indicates a QDA simulation which does not reproduce the width of the $^4He_{g.s.}$ transition. This is due to the Monte Carlo assumed momentum distribution for the nucleons involved in the absorption process, which although fitted to ^4He,$^{16}O(e,e'p)$ data, and scaled for ^6Li via the number of target nucleons, does not include nuclear structure details. The narrowness of the ground state transition was predicted in Ref. [8] to be ≈13°, but could not be measured due to their limited angular coverage.

To obtain the $d\sigma/d\Omega^*$ shown in Fig. 4, the double differential cross sections were fitted with a Legendre polynomial series up to $P_{14}(\cos\theta)$, and integrated. These in turn were also fitted with Legendre polynomials (shown in the figure)

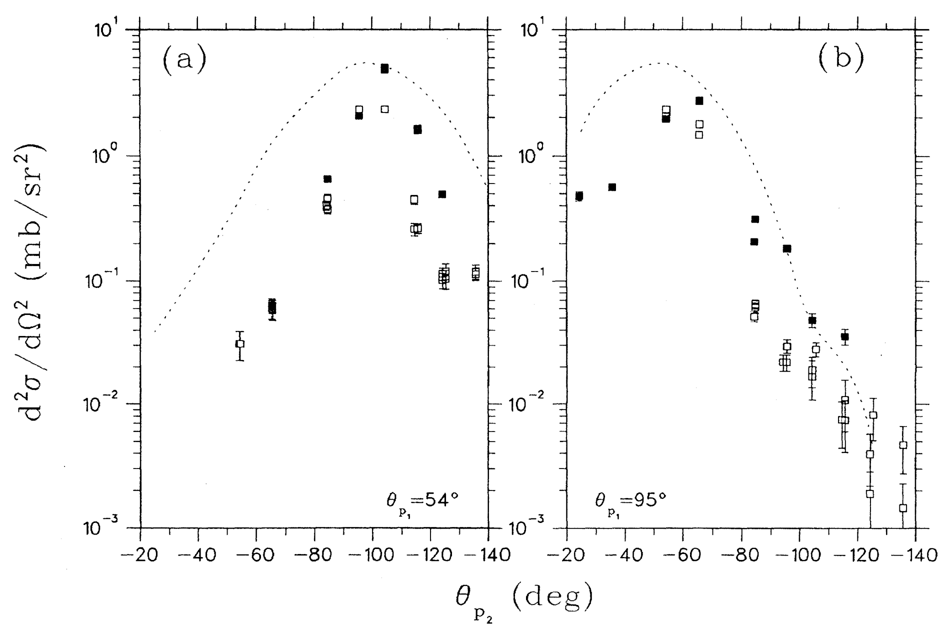

FIG. 3. $d^2\sigma/d\Omega^2$ angular distributions for the $^6Li(\pi^+,pp)^4He_{g.s.}$ reaction at 100 MeV [filled squares] and 165 MeV [open squares]. In both (a), (b) the angle of one assembly is held fixed, while the other is scanned on the opposite side of the beam. The dotted curve is a QDA simulation at 165 MeV, arbitrarily normalized to the data. The difference between the two 100 MeV points in (b) at $\theta_{p_2} = -84°$ is taken into account in the relative systematic errors shown in Fig. 4.

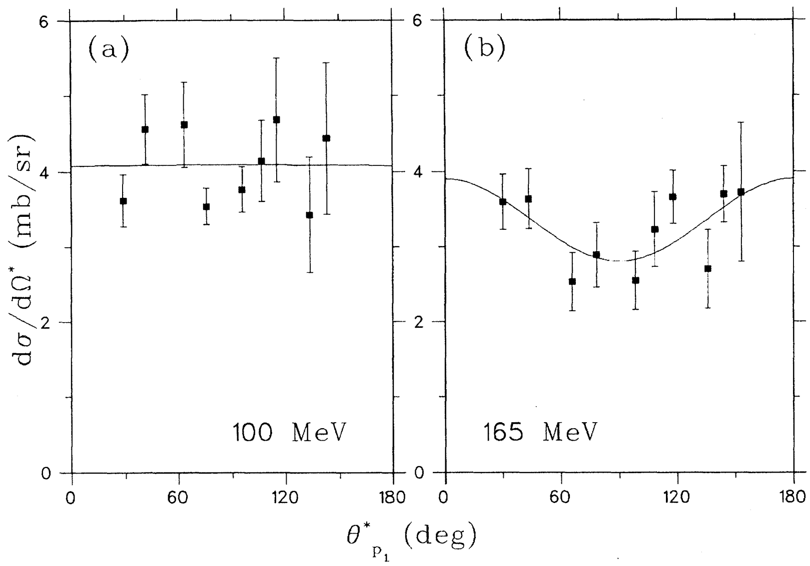

FIG. 4. $d\sigma/d\Omega^*$ angular distributions in the $\pi^+d\rightarrow pp$ center of momentum frame for the $pp+{}^4$He$_{\text{g.s.}}$ final state at (a) 100 MeV and (b) 165 MeV. The smooth curve is a Legendre polynomial fit $P_0+P_2(\cos\theta^*)$.

to provide total cross sections of 12.9$\pm$1.4 at 100 MeV, and 10.0$\pm$1.1 at 165 MeV. These results have had all experimental corrections applied, including reaction losses, edge effects, geometrical acceptance (derived from the Monte Carlo simulations) and energy losses in the target. No corrections have been made for FSI due to the reasons given in the introduction.

Our result at 165 MeV is slightly smaller than at 100 MeV, while the 150 MeV result of [10], and the 115, 140 MeV results of [14] lie between our two values. There is excellent agreement between our result and the result of [14] at 165 MeV. While there is some scatter between the data sets from the different sources, the overall trend is for a cross section that is dropping from 100 to 165 MeV, possibly peaking at a lower energy than the $\pi^+d\rightarrow pp$ reaction (see Fig. 5). This is a surprising result, which can only be understood by looking more closely at the angular distribution information. The pn pair in the initial ^{6}Li state is $l=0$ with respect to the spin-0 ^{4}He core, and since the ^{4}He$_{\text{g.s.}}$ final state is selected, the $l=0$ pp system is therefore favored. Due to momentum transfer considerations, such an angular momentum configuration is more probable at 100 MeV than at 165 MeV. As seen in Fig. 4, the reaction is S wave at 100 MeV, while at 165 MeV the $l=0$ and $l=2$ components interfere destructively near 90°.

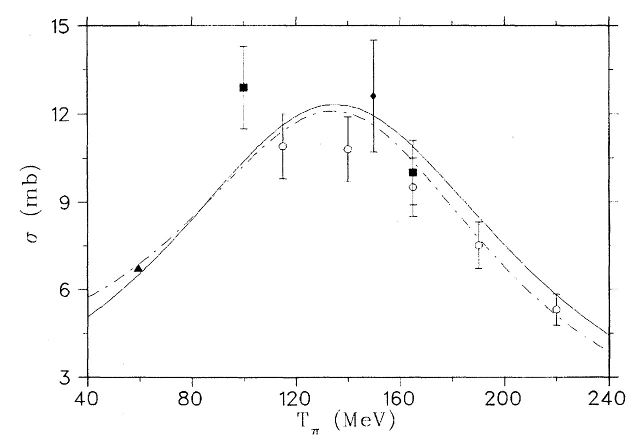

FIG. 5. Total cross sections for the ^{6}Li(π^+,pp)^{4}He$_{\text{g.s.}}$ reaction from [filled squares] this work; [filled triangles] Ref. [8]; [filled diamonds] Ref. [10]; [open circles] Ref. [14]. The solid curve is the parameterization of the $\pi^+d\rightarrow pp$ reaction by Ritchie [20], while the dashed curve is the parameterization by VerWest and Arndt [21]. No scaling factor is applied to these curves, but they are shifted by the 1.5 MeV binding energy of the deuteron within ^{6}Li. The quoted errors for this work include both statistical and relative systematic uncertainties. The absolute systematic error is 15%.

In summary, we have measured the ^{6}Li(π^+,pp)^{4}He$_{\text{g.s.}}$ transition at incident pion energies of 100 and 165 MeV with both good angular granularity and coverage, enabling the angular distribution of the pp correlation to be extracted. The measured width of $\approx$16° (FWHM) at both energies is in reasonable agreement with the prediction of [8] at 59.4 MeV. Total cross sections were obtained by a Legendre polynomial integration of the measured angular distributions. The reaction is found to be essentially $l=0$ at 100 MeV, but contains both $l=0$ and $l=2$ components at 165 MeV. We believe that this causes the cross section at 165 MeV to be slightly smaller than at 100 MeV. It should be also mentioned that a similar energy dependence has been observed recently on ^{3}He, but no explanation was given [22].

We would like to thank Dr. J.L. Visschers for his extensive aid with the Monte Carlo program. This project was supported in part by the Natural Sciences and Engineering Research Council of Canada (NSERC), and the Saskatchewan Department of Economic Development. The generous assistance of Dr. E.W. Vogt is also gratefully acknowledged.

[1] D. Ashery and J.P. Schiffer, Annu. Rev. Nucl. Part. Sci. **36**, 207 (1986).
[2] A. Altman *et al.*, Phys. Rev. C **34**, 1757 (1986).
[3] S.D. Hyman *et al.*, Phys. Rev. C **41**, R409 (1990); **47**, 1184 (1993).
[4] D.J. Mack *et al.*, Phys. Rev. C **45**, 1767 (1992).
[5] B.G. Ritchie, N.S. Chant, and P.G. Roos, Phys. Rev. C **30**, 969 (1984).
[6] P. Weber *et al.*, Phys. Rev. C **43**, 1553 (1991).
[7] D.F. Geesaman *et al.*, Phys. Rev. Lett. **63**, 734 (1989).
[8] R. Rieder *et al.*, Phys. Rev. C **33**, 614 (1986).
[9] E.D. Arthur *et al.*, Phys. Rev. C **11**, 332 (1975).
[10] R.D. Ransome *et al.*, Phys. Rev. Lett. **64**, 372 (1990).
[11] R.D. Ransome *et al.*, Phys. Rev. C **42**, 1500 (1990).
[12] H. Yokota *et al.*, Phys. Rev. C **40**, 1069 (1989).
[13] H. Yokota *et al.*, Phys. Rev. Lett. **58**, 191 (1987).
[14] D. Zhang, Ph.D. thesis, University of Maryland, 1990 (unpublished).
[15] Z. Papandreou *et al.*, Nucl. Instrum. Methods B **34**, 454 (1988).
[16] G.R. Smith *et al.*, Phys. Rev. C **38**, 243 (1988).
[17] J.L. Visschers, in *Proceedings of the International Conference on Monte Carlo Simulation in High Energy and Nucleon Physics*, edited by Peter Dragovitsch, Stephen L. Ninn, and Mimi Burbank (World Scientific, Singapore, 1994), p. 350.
[18] CERN Computer Newsletter **200**, 13 (1990).
[19] G.M. Huber *et al.*, Phys. Rev. C (to be published).
[20] B.G. Ritchie, Phys. Rev. C **28**, 926 (1983).
[21] B.J. VerWest and R.A. Arndt, Phys. Rev. C **25**, 1979 (1982).
[22] T. Alteholz *et al.*, Phys. Rev. Lett. **73**, 1336 (1994).